Rubber-Modified Polystyrene from Multistage Latexes: Rheological and Physical Properties

M. S. SILVERSTEIN and M. NARKIS, *Department of Chemical Engineering, Technion-Israel Institute of Technology, Haifa, 32000 Israel*

Synopsis

The combination of rubbery and rigid polymers in a multiphase structure using staged emulsion polymerization has yielded materials with properties ranging from reinforced elastomers to high impact plastics. The many different particle morphologies that result from multistage latexes include core/shell, domain, interpenetrating polymer networks, and various combinations thereof. The present work focuses on rubber modified polystyrene (polyacrylates (PA) and polystyrene (PS) in a 1 : 3 ratio). The nature of the rubber-modified polystyrene from multistage latexes has been determined through a combination of microscopy and mechanical property analyses. The uncrosslinked PS shells that form around the crosslinked PA seed particles with grafted PS microdomains coalesce upon molding to form a continuous thermoplastic PS matrix that may absorb impact energy through mechanisms of crazing and shear yielding. The crosslinking of the acrylate seed with butadiene enhances PS grafting through residual unsaturation and thus affects the effective particle volume fraction and particle–matrix interaction in these rubber-modified PS materials. The substitution of some of the uncrosslinked PS of the second stage with crosslinked PS in a separate intermediate stage, resulting in a three-stage latex, also affects the effective volume fraction and the particle–matrix interaction through enhanced PS grafting and the formation of interpenetrating networks. In flow the rubber modified PS exhibits a Newtonian plateau at low shear, unlike crosslinked particles which flow through a particle slippage mechanism, and an unexpected deviation from power law behavior at high shear with a viscosity plateau, or even a slight increase in viscosity. These materials may essentially flow through molecular deformation, depending upon the temperature, molecular weight, particle–matrix interaction, and level of shear. The rubber-modified PS from the multistage latexes are a potential high impact material whose unique structure and chemistry distinguish it from commercial high impact PS (HIPS), although its mechanical and impact properties are, at the very least, similar to those of HIPS.

INTRODUCTION

The unique and sometimes synergistic properties of high-impact plastics such as high-impact polystyrene (HIPS), acrylonitrile–butadiene–styrene (ABS), and styrene–butadiene block copolymers result from the combination of two polymers with different properties in a multiphase structure.[1-3] The combination of two polymers, one rubbery and the other rigid, can yield materials with properties ranging from reinforced elastomers to high-impact plastics. The superior properties of these materials depend upon compatibility, polymerization technique, composition, crosslink density, and processing. Many different polymers and methods of synthesis have been combined to create high-impact plastics, the most common of which are HIPS and ABS.

HIPS may be synthesized through the bulk or bulk/suspension polymerization of styrene in the presence of dissolved polybutadiene (PBD) rubber. During the stirred bulk prepolymerization of styrene used in both processes, the dissolved rubber is grafted with polystyrene (PS), crosslinks, phase separates,

Journal of Applied Polymer Science, Vol. 40, 1583–1599 (1990)
 CCC 0021-8995/90/9-101583-17$04.00

and yields rubbery particles on the order of 1–10 μm which also contain some grafted PS phase-separated domains.[4] The PBD content in HIPS is limited to approximately 12% by the high solution viscosity of the polymerization process and the limited solubility of rubber in styrene.[3] The emulsion polymerization of styrene–acrylonitrile (SAN) monomer mixture in the presence of 0.1 μm rubbery particles from a PBD seed latex yields particles whose morphology is that of a rubbery crosslinked PBD core with grafted SAN microdomains surrounded by a SAN shell.[5]

The effective volume fraction of the rubber particles in these materials includes the volume fraction of the rubber, grafted glassy domains, and rigid polymer grafted to the particle's surface. Both the rubbery particle and the grafted rigid polymer contribute to the overall nature of the rubbery particle in the matrix and the particle–matrix interaction.[3] The formation of a shell of grafted rigid polymer around the rubbery particles prevents particle aggregation in the molded high impact materials, enhances matrix–particle interaction, and thus is critical to their superior impact properties.[3,6,7] The effective volume fraction thus increases with the grafting of the rigid polymer to the rubbery particle. The influence of grafting upon the effective volume fraction is more significant in the 0.1 μm rubbery particles of ABS than in HIPS due to the larger area to volume ratio of the ABS particles. A minimum in effective particle volume fraction exists in ABS, however, due to the particle aggregation which traps ungrafted molecules and yields an increase in effective volume when there is not enough grafted rigid polymer to promote particle–matrix interaction. Optimum properties may be realized in HIPS and ABS through the variation of the effective particle volume fraction, particle composition (concentration of grafted rigid polymer in the rubbery particle), rubber crosslinking, and particle size (area to volume ratio at a given effective volume fraction). The energy absorption mechanisms of crazing and shear banding can yield significantly improved impact properties at optimum parameters with a tolerable decrease in tensile stiffness and strength.[3,7–9]

The glass transition temperature and height of the loss tangent peak in HIPS both increase with the effective particle volume fraction, the concentration of grafted PS in the particles (particle composition), and rubber crosslinking. These increases exhibited in the dynamic properties are also reflected in the impact energy absorption of high impact plastics, which increases with effective particle volume fraction.[3] In both HIPS and ABS the particle–matrix interaction is crucial to the energy absorption mechanism in order to prevent particle dewetting. HIPS absorbs energy mainly through a mechanism of crazing, and thus the impact energy absorption is more sensitive to the particle size in HIPS than it is in ABS. There is a significant increase in melt viscosity in high impact plastics with increasing effective particle volume fraction and increasing particle area to volume ratio (decreasing particle size). A glassy polymer with a molecular weight lower than its commercial equivalent forms the thermoplastic matrix in a high impact plastic to compensate for the viscosity increase resulting from rubber modification.[3]

The two-stage emulsion polymerization procedure used to synthesize ABS can, in fact, generate various particle morphologies including core/shell (C/S), inverted C/S, domain, interpenetrating polymer networks (IPN), and various combinations thereof.[10–13] Minimal grafting and crosslinking may result in an eventual phase separation into a dumbbell structure. The particle mor-

phology is determined by the synthesis technique, physical properties of the monomers and polymers, composition, and monomer/polymer interactions.[14-20] The molded material's structure and properties are determined by the particle morphology, molding technique, and processing history. Swelling of the seed, polymerization (and copolymerization), crosslinking, phase separation, molecular entanglement, and grafting may all occur simultaneously within a monomer/polymer particle emulsified in an aqueous medium. Electron microscopy of ABS has revealed that at low SAN conversions the crosslinked rubbery polybutadiene latex particles contain grafted SAN microdomains, with a profusion of domains upon the particle's surface.[5] At higher SAN conversions the SAN surface domains form a shell around the rubbery particles filled with SAN domains.

A high-impact polystyrene with unique properties and morphologies can also be synthesized through a two-stage latex (TSL) synthesis, using a crosslinked emulsion polymerized polymer I as a seed latex for a subsequent second stage emulsion polymerization of monomer II. Both the particle structure and the structure of the molded material affect the properties of TSL materials.[21-25] The purpose of this research is to examine the effects of the concentration of seed crosslinker and the effects of the fraction of glassy polymer which undergoes crosslinking upon the properties of a rubber-modified PS (RM-PS). Specifically, this RM-PS is based upon a multistage latex where, in the final stage, styrene is polymerized either upon a seed latex of crosslinked rubbery polyacrylate (PA) from the first stage or upon a two-stage latex resulting from the polymerization of styrene and a crosslinker upon a stage I PA seed latex. The PA crosslinker will not only affect the PA crosslink density but will also affect the effective volume fraction, particle composition, and particle–matrix interaction through enhanced PS grafting. The substitution of crosslinked PS (xPS) for some of the PS not only enhances the grafting but may also yield enhanced mixing of the crosslinked PS network with the crosslinked PA (xPA) network through the formation of entanglements and an intertwined structure. In these materials the particles, comparable in size to those used in ABS and much smaller than those that result from HIPS polymerization, are contained within the PS matrix whose molecular weight from emulsion polymerization is significantly greater than that used in commercial HIPS.

EXPERIMENTAL

The emulsion polymerization procedure used in each of the stages follows standard synthesis techniques.[16,26,27] Each stage consisted of a semibatch reaction with both organic and aqueous feeds to the reaction vessel. Stage I in the synthesis procedure was the polymerization and crosslinking of the acrylate to be used as a seed polymer. The acrylate was a mixture of 70% butyl acrylate (BA) and 30% ethyl acrylate (EA), crosslinked with butadiene (BD). Stage II and stage III in the sequential polymerization were the polymerization of styrene added to the latex from the previous stage. In a synthesis with three stages divinylbenzene (DVB) was added to the styrene as a crosslinking agent at 0.25 mass % of the styrene in stage II.

The series of polymerizations in Table I, series I, was synthesized in order to determine the effects of the concentration of BD, the PA crosslinker, upon

TABLE I
Series I—Two-Stage Latex Synthesis[a]

	Stage I		Stage II
	PA	BD	PS
No.	(mass %)		(mass %)
1	25	0.0	75
2	25	1.5	75
3	25	3.0	75
4	25	4.5	75

[a] PA = stage I monomer (butyl acrylate : ethyl acrylate = 70 : 30), % of total monomers; BD = stage I crosslinker (butadiene), % of stage I monomer; PS = stage II and stage III monomer (styrene), % of total monomers.

the mechanical and rheological properties. The series of polymerizations in Table II, series II, was synthesized in order to determine the effects of the substitution of xPS for some of the PS upon the mechanical and rheological properties. Series I maintained a constant composition (25PA/75PS) with the concentration of BD in the acrylate varied. Series II maintained a constant concentration of 3.0 mass % BD in the acrylate in stage I and a constant overall composition (25xPA/75PS) with the ratio of crosslinked PS to total PS varied. The xPS content in the rubbery particles from a 25xPA/8.3xPS/66.7PS three-stage latex is 25%, while the xPS content in the rubbery particles from a 25xPA/25xPS/50PS latex is 50%.

The latexes were coagulated through the addition of methanol. The excess methanol was removed through centrifugation. The resulting material was dried overnight at 40°C in a vacuum oven. Samples were then compression-molded at 20 MPa and 180°C.

The mechanical properties at various temperatures were determined with an Instron tensile tester at a crosshead speed of 10 cm/min on compression-molded strips.

The rheological properties were determined with an Instron capillary rheometer, whose shear rate varied from 0.05 to 500 s^{-1} through the variation of its piston speed. The dynamic viscosity was studied using parallel plate vis-

TABLE II
Series II—Three-Stage Latex Synthesis[a]

	Stage I		Stage II		Stage III
	PA	BD	PS	DVB	PS
No.	(mass %)		(mass %)		(mass %)
3	25	3.0	75.0	0.00	0.0
5	25	3.0	8.3	0.25	66.7
6	25	3.0	25.0	0.25	50.0

[a] DVB = stage II crosslinker (divinylbenzene), % of stage II monomer. See footnote to Table I for other abbreviations.

cometry (Rheometrics System 4 DMS) at low strains and at temperatures above 100°C (a normal force was maintained on the samples to prevent distortion).

The T_g's of the TSL were determined with a temperature sweep from −100 to 160°C using both dynamic mechanical spectroscopy (Rheometrics System 4 DMS in either torsion or parallel plate geometries at low frequencies and strains) and differential scanning calorimetry (Mettler DSC).

Polymer samples enclosed in sealed extraction thimbles were placed in boiling toluene for 2 weeks. The gel content is the ratio of the weight of the polymer remaining to the weight of the original sample.

Thin frozen specimens for a cold-stage TEM procedure[28–31] were prepared using the double-film technique in which a layer of diluted latex of less than 0.5 μm thick was sandwiched between two polyimide-film-covered grids and frozen in liquid nitrogen. The frozen latex samples were examined with 100 kV electron beam at 95 K by finding a suitable area at low magnification and recording a series of micrographs at 20,000 × until approximately 5 min had elapsed, corresponding to electron exposures (doses) of 2–30 kC/m^2.

RESULTS AND DISCUSSION

The two-stage latex procedure used to synthesize the RM-PS materials from PA and PS is similar to the synthesis route used by the authors for PA/PS elastomeric latex interpenetrating polymer networks (LIPN). In LIPN, however, the monomer in both stages of the polymerization contains a crosslinking agent.[21–25] Electron microscopy and mechanical properties have revealed the effects of composition upon the morphology of these soft LIPN particles. At 75% lightly crosslinked polyacrylate (xPA) there exists an interpenetrating network-domain structure. At higher xPS concentrations, however, lightly crosslinked xPS-rich shells are formed around the LIPN particles. Interestingly, the formation of xPS-rich shells on 150 nm xPA seed particles at 35% xPS does not occur simultaneously on all the xPA particles. An increased styrene affinity for particles already containing PS yields, in the second stage, a state of preferential polymerization. The xPS-rich shells increase the PS continuity and gradually eliminates the crosslinked xPA continuity in the molded material. At 50% xPS all the LIPN particles have xPS-rich shells.[21–23] The particle identity is maintained in these shelled LIPN which flow through a particle slippage mechanism insensitive to molecular weight.

The synthesis of the RM-PS differs in that, contrary to the elastomeric LIPN, the PS is uncrosslinked and is the major component, comprising 75% of the multistage latex. The RM-PS latex particles may flow through a molecular deformation mechanism whereupon their flow behavior becomes molecular-weight-dependent, contrary to the particle flow mechanism which is sensitive to friction between particles and slip at the wall. The variation in BD concentration in the acrylate in the TSL elastomers affects the composition of the crosslinked particles through the formation of a grafted PS IPN-microdomain morphology.[21,23,24] The addition of a crosslinker to the PS has been used in these elastomeric TSL to enforce some mixing of incompatible PA and PS through the formation of an interpenetrating network structure.[21,23,24] Thus the addition of a crosslinker to some of the PS in the RM-PS by using a three-

stage polymerization procedure with only the stage II PS crosslinked may form a similar structure and thus affect the composition of the rubbery crosslinked particles, the dispersed phase in the thermoplastic PS matrix.

Electron microscopy and mechanical property studies have revealed the relationships between the synthesis, morphology, and impact resistance of HIPS and ABS.[3] The degree of crosslinking, particle composition (concentration of grafted rigid polymer), particle size, and effective volume fraction, which have a significant influence upon the morphology and properties of high impact plastics such as HIPS and ABS, should similarly affect the RM-PS. The behavior of the particles in a frozen latex under electron beam irradiation has been used previously to distinguish between polymers that undergo scission and polymers that crosslink.[28-31] Cold stage TEM examination of a frozen RM-PS (Fig. 1) has revealed a bimodal particle size distribution. The swelling and cellular appearance of the smaller 60 nm particles is typical of xPA while the stability of the larger 300 nm particles is typical of PS particles or particles with a PS-rich shell.[22-24] During the polymerization the presence of PS in some of the 60 nm xPA seed particles increases their affinity to styrene and results in further preferential styrene polymerization within them. Preferential styrene polymerization, already observed in the larger 150 nm particles of the 35% xPS TSL,[21] may be enhanced by the sensitivity of the phenomenon to the greater area to volume ratio in the 60 nm xPA seed particles of the RM-PS and yields the bimodal distribution. The schematic diagram in Figure 1 illustrates the PS phase separation into grafted microdomains at low PS concentrations followed by the formation of a PS-rich shell yielding a C/S-like particle. The PS shells in these particles coalesce upon molding, forming a continuous PS matrix containing a discrete dispersion of rubbery xPA particles containing grafted PS microdomains.

The effect of crosslinking upon the gel content in homopolystyrene and homopolyacrylate latexes is to increase the gel content from approximately

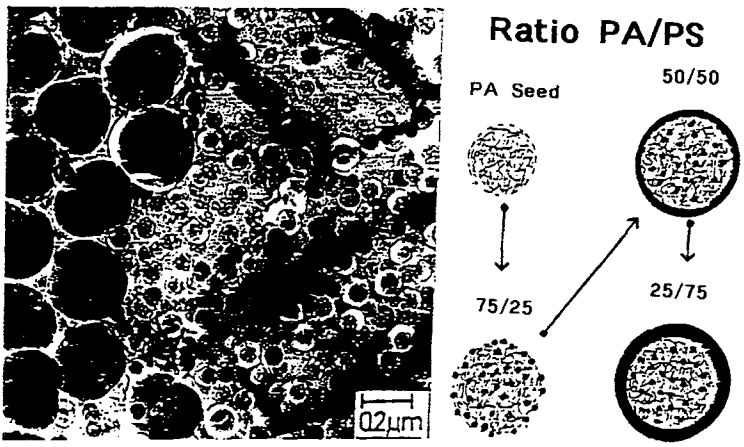

Fig. 1. Transmission micrograph of frozen 25xPA/75PS TSL exhibiting a bimodal particle distribution. The smaller particles (60 nm) behave like PA under electron beam irradiation while the larger particles (300 nm) behave like PS or PS-rich shelled particles. Accompanying schematic illustration depicts hydrophilic crosslinked PA seed with PS microdomains within the particle which is eventually covered by a PS-rich shell at high PS compositions.

zero for the uncrosslinked homopolymers to 60% for PA crosslinked with 3% BD and 50% for PS crosslinked with 0.25% DVB. A 75PA/25xPS TSL elastomer with no BD in the PA seed should thus have a gel content of approximately 13% through PS crosslinking alone. The 65% gel content found in this 75PA/25xPS TSL therefore reflects a significant grafting reaction that occurs between the high molecular weight PA seed and the crosslinked PS network.[21,32-34] An increase to 90% gel in a 75xPA/25xPS TSL elastomer, whose gel content would be approximately 58% from PA and PS crosslinking alone, reflects the presence of the BD, which crosslinks the PA and enhances PS grafting to the PA network through residual BD unsaturation.[21] The ratio of grafted PS to total PS increases with increasing PA content, emphasizing the importance of the PA concentration in this grafting reaction. The dominance of the PA in this grafting reaction is also reflected in the fact that there is no grafting reaction when a PS seed is used in a PS/PA TSL.[21,33,35]

The bimodal distribution in the RM-PS in Figure 1 has revealed that the greater part of the PS forms thick shells on the 60 nm xPA seed particles, and the significant grafting of PS to the PA network may be restricted to these C/S-like particles. When neither the PS nor the PA is crosslinked, there is no crosslinked network in the particles and the PA, PS, and PS-grafted PA are dissolved by toluene, resulting in a gel content of zero, as seen in Figure 2(a). The presence of BD, which crosslinks the PA and enhances the grafting of the uncrosslinked PS to the PA network, yields the significant gel content in Figure 2(a). The gel content of 31% in the RM-PS with 3.0% BD in the acrylate seed in Figure 2(a) is twice that expected from PA crosslinking alone due to the enhanced grafting of the high molecular weight PS. The addition of crosslinked PS to the xPA seed and the formation of grafted, entangled, and interwoven crosslinked networks with grafted PS microdomains is seen in Figure 2(b) to yield a significant increase in the gel content. The gel content is determined by the degree of PA crosslinking, degree of PS crosslinking, and degree of the grafting in the networks. The latter two factors reflect the effective volume fraction, particle composition, and particle–matrix interaction, all of which may affect the mechanical properties of the RM-PS.

The PS-like storage modulus of an RM-PS with 3% BD in the PA seed in Figure 3(a) from the dynamic mechanical spectrometry studies indicates the PS continuity in these materials. The storage modulus of the RM-PS is greater than that of the 50xPA/50xPS TSL whose PA continuity has been diminished by the PS-rich shells which partially coalesce upon molding. The loss tangent peak of the RM-PS is closer to the T_g of the PA homopolymer than that of the 50xPA/50xPS TSL. This shift in the peak reflects the reduction in the grafting of PS to the xPA network with the reduced PA content, the bimodal particle size distribution with the relatively PS-free xPA particles, and the inability of the uncrosslinked PS to form an IPN structure that enhances molecular mixing.[35] Both the complex viscosity and storage modulus of the RM-PS in Figure 3(b) are an order of magnitude greater than those seen for the xPS-rich shelled 50xPA/50xPS TSL. The molded 50xPA/50xPS TSL flows through interparticle friction and slippage, while the thermoplastic RM-PS high molecular weight PS matrix flows through molecular deformation, yielding the higher molecular-weight-dependent viscosity in the RM-PS.

The viscosity curves in Figure 4(a) at 150°C for the RM-PS with various degrees of seed crosslinking exhibit the same basic shape. A power law region

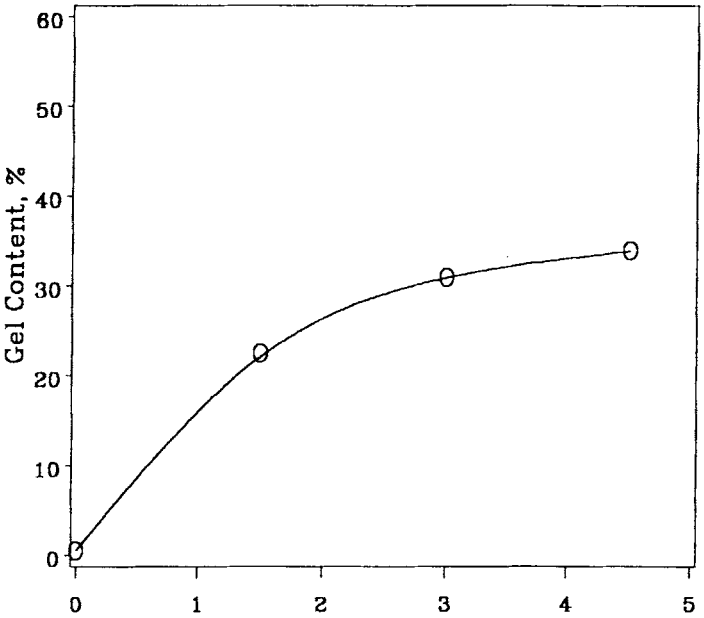

(a)

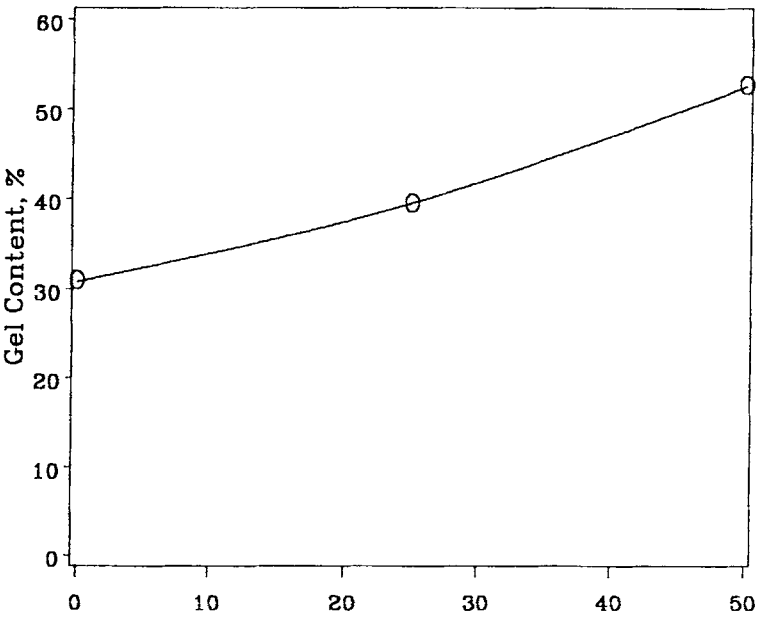

(b)

Fig. 2. Gel content of RM–PS: (a) crosslinker in acrylate varied (BD by mass), composition constant (25PA/75PS); (b) xPS content in particle varied, overall composition 25xPA/75PS, 0.25% DVB in fraction of styrene to be crosslinked, and 3.0% BD in acrylate.

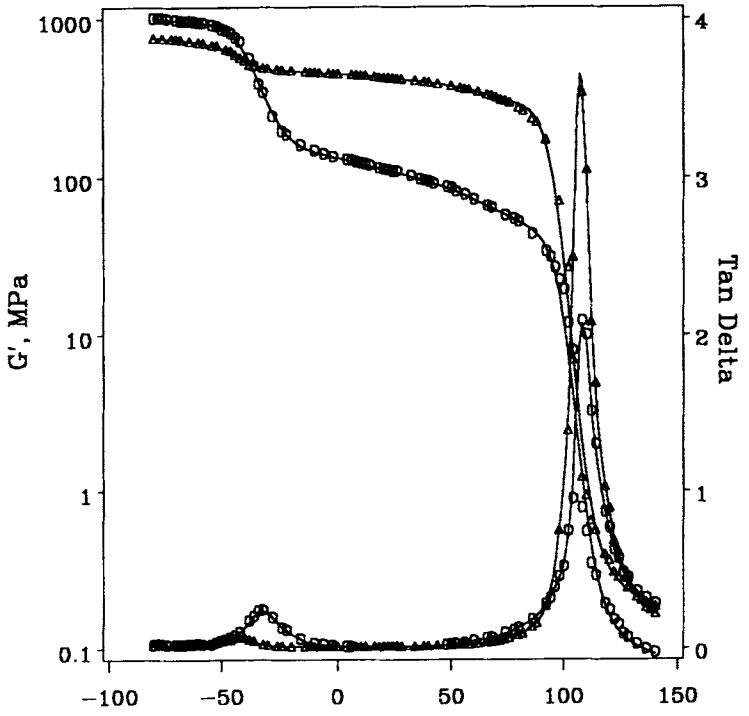

(a)

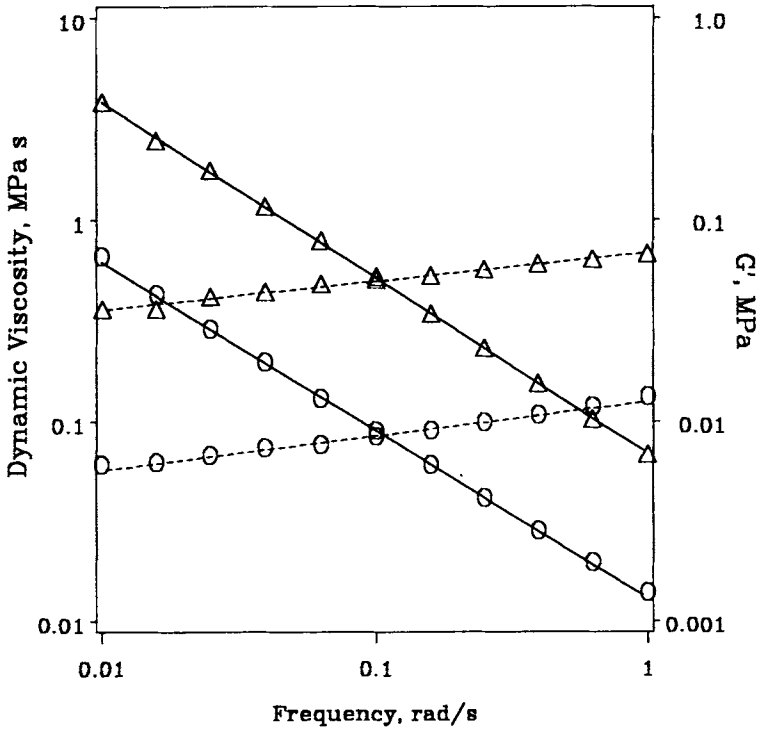

(b)

Fig. 3. Dynamic properties of an RM-PS and a shelled LIPN: (○) 50xPA/50xPS; (△) 25xPA/75PS; (a) temperature sweep in torsion and parallel plate test geometries; (b) frequency sweep using parallel plate at 150°C; (——) dynamic viscosity; (– – –) G'.

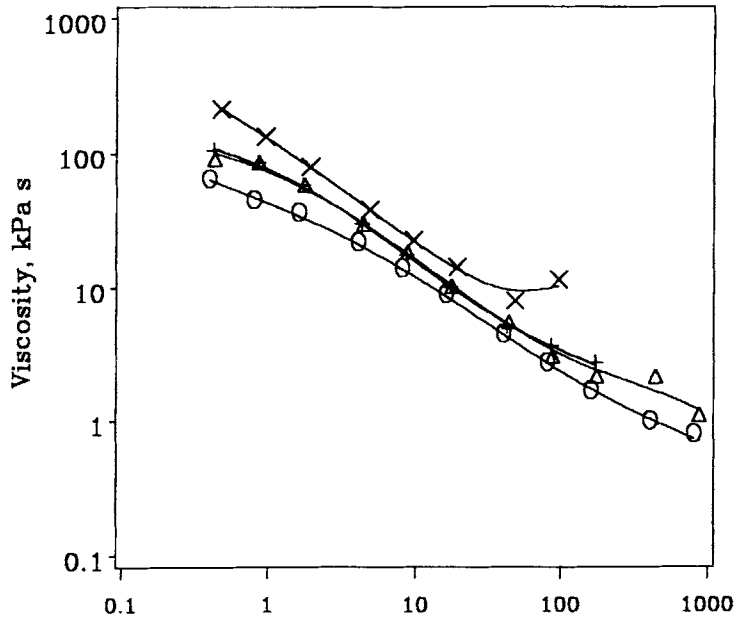

(a)

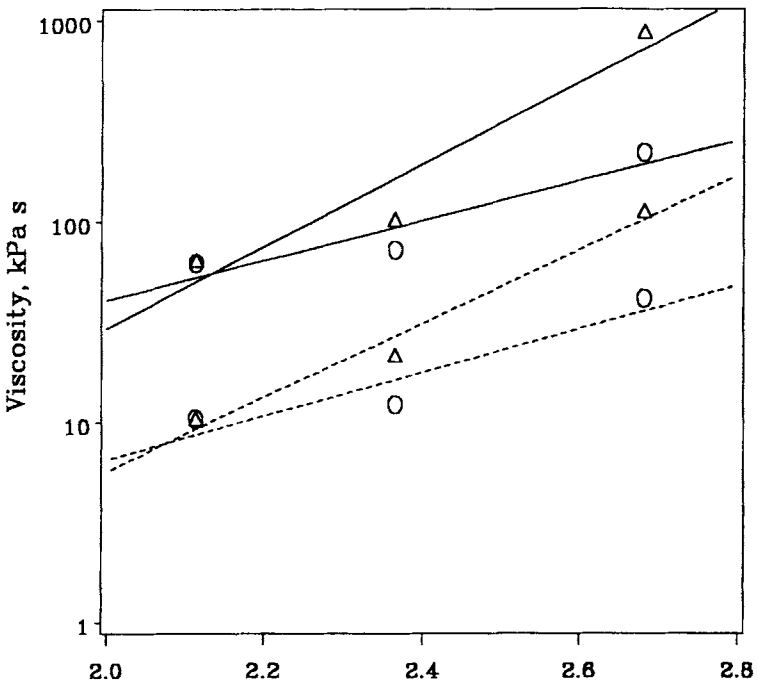

(b)

Fig. 4. Capillary rheometer flow curves of RM-PS. (a) crosslinker in acrylate varied (BD by mass), composition constant (25PA/75PS), at 150°C: (○) 0.0%; (△) 1.5%; (+) 3.0%; (×) 4.5%. (b) Activation energy of flow at constant shear rate (the slope reflects the flow mechanism): (○) 50xPA/50xPS; (△) 25xPA/75PS. (——) 0.1 s^{-1}; (- - -) 1.0 s^{-1}. (c) Various methods of 25xPA/75PS latex synthesis at 200°C: (○) TSL; (△) latex mixture; (+) emulsion copolymerization.

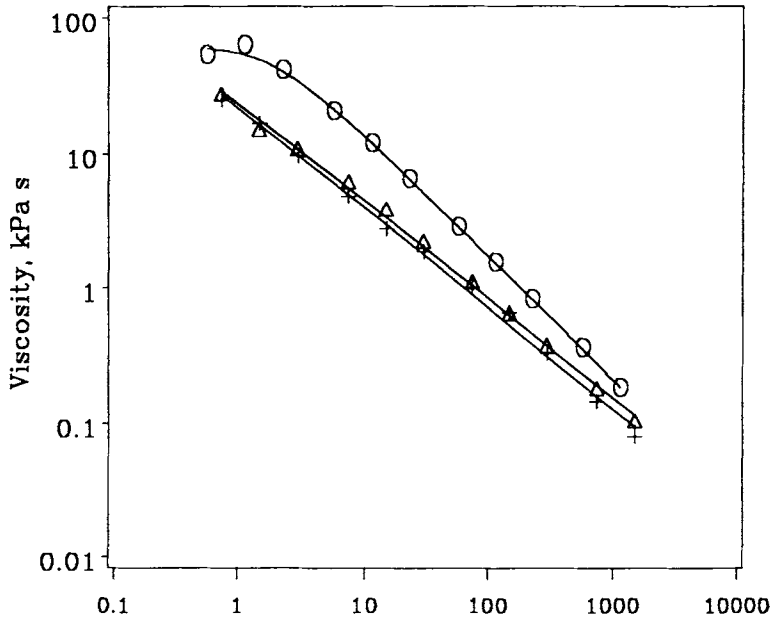

(c)

Fig. 4. (*Continued from previous page.*)

is evident, as is an approaching Newtonian plateau at the lowest shear rates studied. The elastomeric LIPN with 25–50% xPS, which flow by a particle flow mechanism that is not affected by molecular weight, exhibit no Newtonian plateau at the same low levels of shear rates.[21,23,36] The PS is not crosslinked in these RM-PS materials and the flow through molecular deformation of the RM-PS and similar high impact materials, such as ABS, can be modeled taking the crosslinked rubbery particles into account.[37] The increase in viscosity with the concentration of BD in the xPA seed in Figure 4(a) results from the increase in the effective rubber particle volume fraction due to PS grafting and a corresponding increase in particle–matrix interaction.[3]

The flow activation energy at constant shear rates of the RM-PS materials from the slopes of the Arrhenius plot in Figure 4(b) is twice that of the PS-rich shelled 50xPA/50xPS LIPN elastomers due to the difference between the flow mechanisms. The flow mechanism in these RM-PSs thus depends upon the temperature, molecular weight, and level of shear. The high molecular weight of the emulsion-polymerized PS is an important factor in the molecular flow mechanism (as opposed to the insensitivity of the particle flow mechanism to the molecular weight) yielding a significantly high viscosity. The lower viscosity and power law behavior at 200°C in Figure 4(c) of a polymer resulting from a latex mixture and a latex copolymer whose composition is identical to that of the 25xPA/75PS TSL (exhibiting the approaching Newtonian plateau at low shear) results from the greater effective particle volume fraction, increased particle–matrix interaction, and larger area to volume ratio of the 60 nm particles in the RM-PS, as well as the different flow mechanisms.

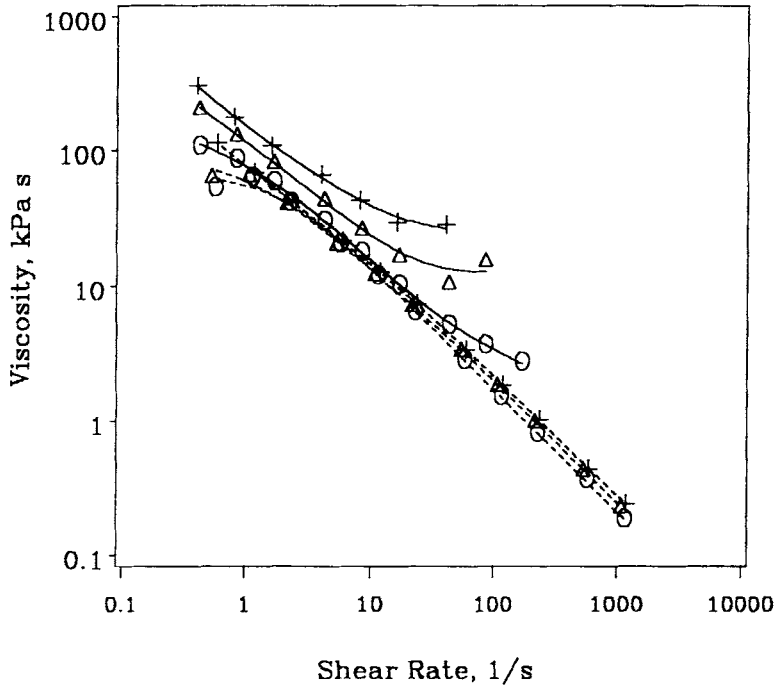

(a)

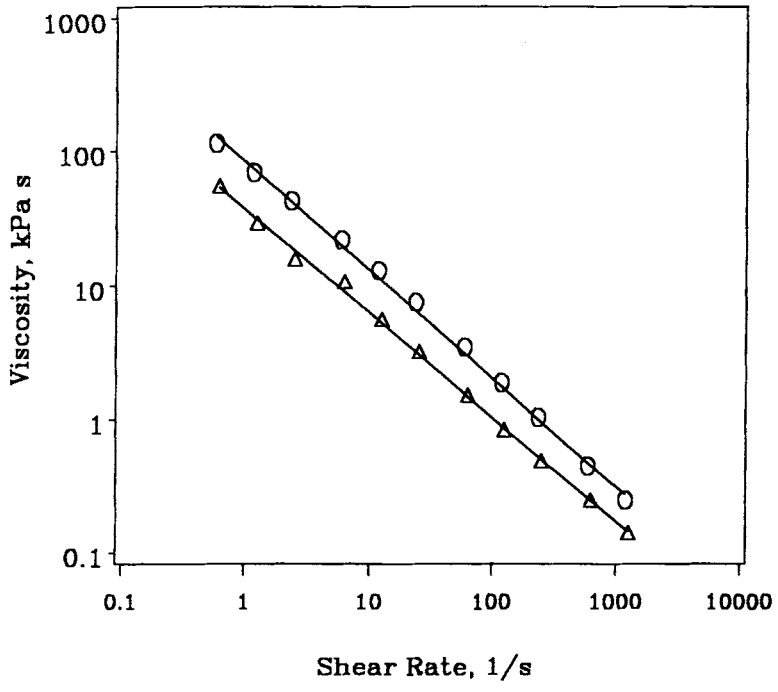

(b)

Fig. 5. Capillary rheometer flow curves of RM-PS. (a) xPS content in particle varied, overall composition 25xPA/75PS, 0.25% DVB in fraction of styrene to be crosslinked, and 3.0% BD in acrylate: (○) 0%; (△) 25%; (+) 50% (+) 50%; (——) 150°C; (---) 200°C. (b) Various methods of 25xPA/25xPS/50PS latex synthesis at 200°C: (○) three-stage latex; (△) latex mixture.

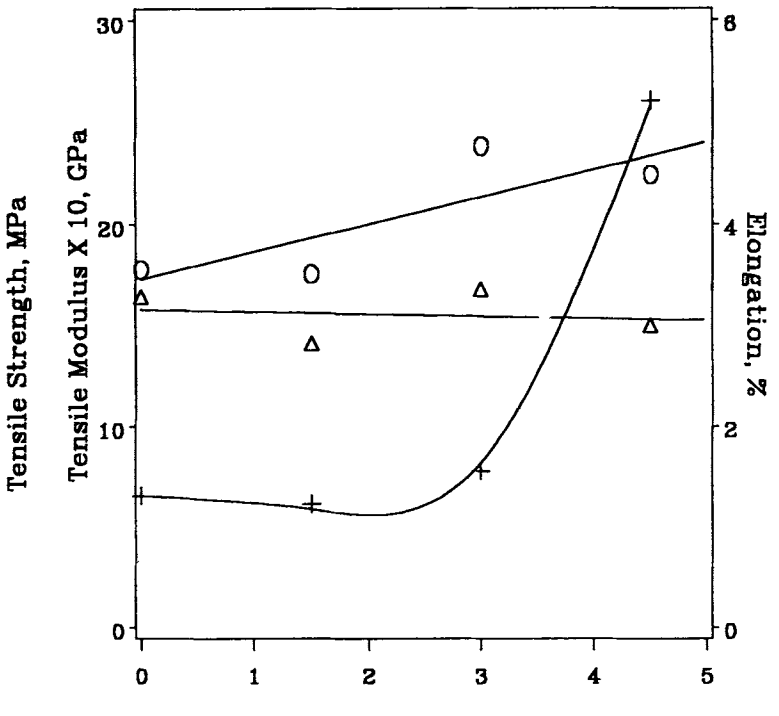

(a)

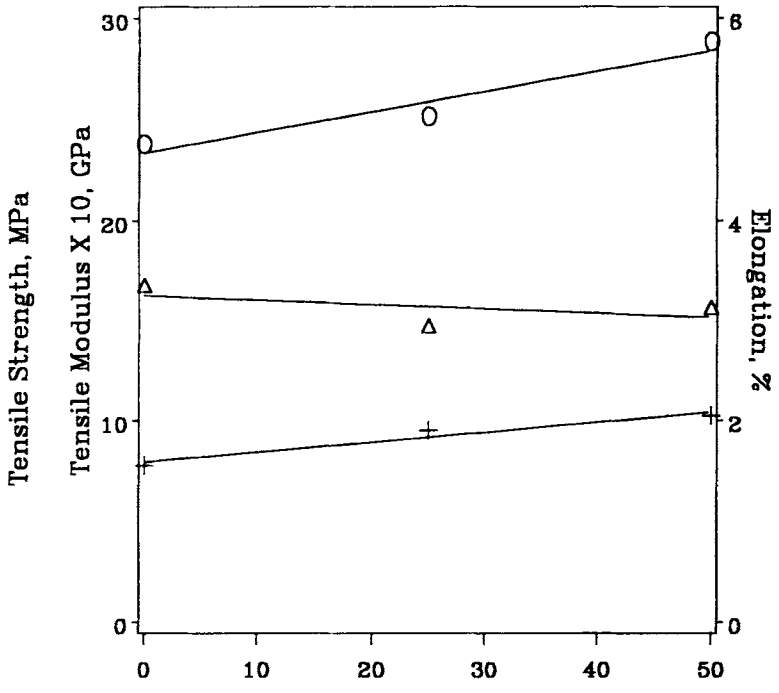

(b)

Fig. 6. Tensile properties of RM-PS TSL: (○) tensile strength; (△) tensile modulus; (+) elongation. (a) Crosslinker in acrylate varied (BD by mass), composition constant (25PA/75PS). (b) xPS content in particle varied, overall composition 25xPA/75PS, 0.25% DVB in fraction of styrene to be crosslinked, and 3.0% BD in acrylate.

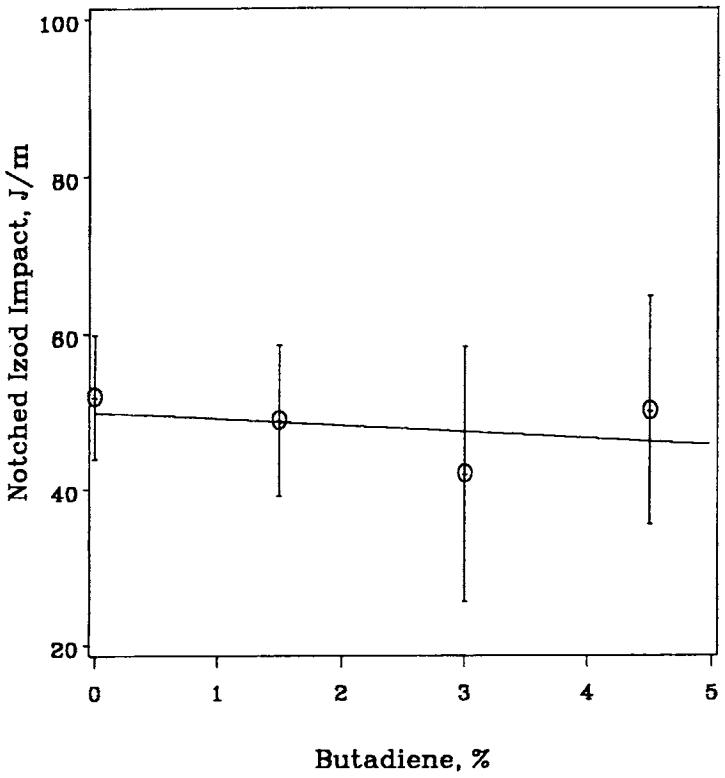

Fig. 7. Notched Izod impact energy for RM-PS. The error bars indicate the standard deviation, $\pm \sigma$, from the mean. (a) Crosslinker in acrylate varied (BD by mass), composition constant (25PA/75PS). (b) xPS content in particle varied, overall composition 25xPA/75PS, 0.25% DVB in fraction of styrene to be crosslinked, and 3.0% BD in acrylate.

The formation of an entangled crosslinked PS network and the increase in grafting yields an increase in the effective volume fraction, PS content in the particle, and particle–matrix interaction.[3] These factors result in the increase in viscosity in Figure 5(a) with increasing xPS in the latexes, both at 150 and 200°C. The approaching Newtonian plateau at 150°C at the lowest shear rates studied is less discernable in the RM-PS with increasing xPS content. The Newtonian plateau is more pronounced at 200°C, a temperature much greater than the PS T_g. The lower viscosity of a mixture of homopolymer latexes of the same composition as an RM-PS (25xPA/25xPS/50PS) in Figure 5(b) reflects the larger effective particle volume fraction, increased particle–matrix interaction, and larger area to volume ratio of the 60 nm particles in the RM-PS, as well as differences in the flow mechanisms.

The molecular-weight-dependent flow mechanism is also responsible for the deviation from power law behavior with a viscosity plateau, or even a slight viscosity increase, at high shear rates. The viscosity plateau, or slight increase in viscosity, seen at 150°C in Figures 4(a) and 5(a) is exhibited at even lower shear rates at 100°C.[21] This effect occurs in the RM-PS at decreasing shear rates as the effective particle volume fraction and particle–matrix interaction is increased by the increasing concentrations of BD or xPS, as seen in Figures 4(a) and 5(a). This viscosity plateau is not observed at 200°C in Figure 5(a),

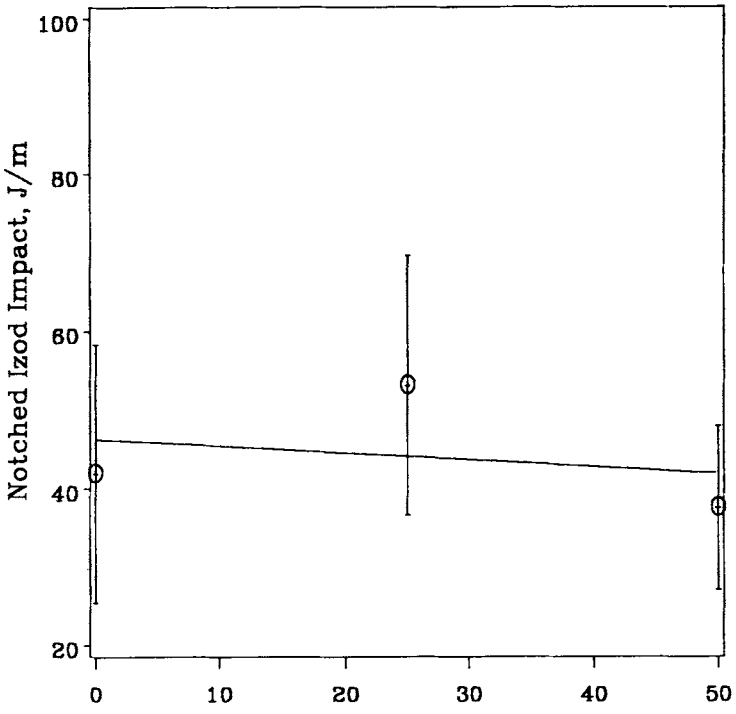

(b)

Fig. 7. (*Continued from previous page.*)

a temperature significantly above the PS T_g. An increase in the glass transition of PS due to pressure effects at high levels of shear and temperatures close to the PS T_g has been reported to affect the viscosity and yield similar deviations from power law behavior in PS.[38,39] A theoretical viscosity curve, not shown, that takes the pressure effect into account closely follows the experimental results in Figures 4(a) and 5(a). The viscosity correction is based upon the relationship between the pressure and the increase in T_g, using the WLF equation to find a shift factor from the glass transition temperatures that accounts for the increase in viscosity.[38,39]

The increase in tensile strength in Figure 6(a) reflects the increased particle–matrix interaction due to the increase in grafting. The increase in elongation in Figure 6(a), which at 4.5% BD is significantly greater than that of commercial PS, reflects the increasing effective particle volume fraction and the improved particle–matrix interaction. These effects are also exhibited by the increasing tensile strength with the substitution of some of the PS by xPS in Figure 6(b). The tensile modulus in both Figures 6(a) and 6(b) is relatively unaffected by these factors, with the overall composition and basic structure maintained constant in these RM-PSs. The large scatter and standard deviation of the notched Izod impact results in Figures 7(a) and 7(b) yield little information about the effects of BD concentration in the acrylate and fraction of total PS replaced by xPS in these RM-PSs.

The average impact energy (45 J/m), tensile strength (25 MPa), and tensile modulus (1.5 GPa) in these RM-PSs are of the same order of magnitude as

those in HIPS. The TSL synthesis, however, differs in that a significantly greater mass fraction of rubber is included within the high molecular weight PS matrix in particles much smaller than those that result from HIPS synthesis. The control of grafting and the formation of an IPN structure can be used to find an optimum in particle–matrix interaction in these RM-PSs, which are potential high impact materials. The suppression of the preferential styrene polymerization for example, through the use of xPA seed particles of approximately 150 nm instead of 60 nm, will yield a more uniform C/S latex that will also improve the uniformity of the grafting/IPN formation, reduce viscosity through the particle's reduced area to volume ratio, and more effectively use the rubbery particles for impact absorption while minimizing the loss of tensile properties.

CONCLUSIONS

- Rubber modified PS can be synthesized using a multi-stage emulsion polymerization procedure whose first stage is a rubbery PA latex.
- Upon molding the PS shells coalesce and form a continuous thermoplastic matrix which interacts with the lightly crosslinked rubbery particles which retain their identity and act as a filler.
- The flow of the thermoplastic PS matrix, essentially through molecular deformation, is molecular weight sensitive, unlike the flow by particle slippage of latex IPN and crosslinked PS shelled latex IPN.
- A Newtonian plateau at low shear rates and an unexpected deviation from power law behavior with a viscosity plateau, or a slight increase in viscosity, at high shear rates are noted in the rubber modified PS. These phenomena depend upon the temperature and level of shear.
- The butadiene crosslinking of the acrylate in the seed enhances PS grafting through residual unsaturation and yields an increase in the effective particle volume fraction and the particle–matrix interaction.
- The addition of divinylbenzene to some of the styrene in a second stage enhances PS grafting and the formation of interpenetrating networks and yields an increase in the effective particle volume fraction and the particle–matrix interaction.
- The rubber modified PS synthesized through multistage latex emulsion polymerization has impact and mechanical properties that are, at the very least, similar to those of HIPS.

References

1. D. R. Paul and S. Newman, *Polymer Blends,* Academic, New York, 1978.
2. J. A. Manson and L. H. Sperling, *Polymer Blends and Composites,* Plenum, New York, 1976.
3. C. B. Bucknall, *Toughened Plastics,* Applied Science, London, 1977.
4. R. J. Williams and R. W. A. Hudson, *Polymer,* **8,** 643 (1967).
5. K. Kato, *Jpn. Plast.,* **2,** 6 (1968).
6. Y. Aoki, *Macromolecules,* **20,** 2208 (1987).
7. H. Keskkula, D. R. Paul, K. M. McCreedy, and D. E. Henton, *Polymer,* **28,** 2063 (1987).
8. S. Y. Hobbs, *Polym. Eng. Sci.,* **26,** 74 (1986).
9. C. D. Han, *Polymer Blends and Composites in Multiphase Systems,* American Chemical Society, Washington, DC, 1984, p. 221.
10. D. I. Lee and T. Ishikawa, *J. Polym. Sci., Polym. Chem. Ed.,* **21,** 147 (1983).

11. R. A. Dickie, M. F. Cheung, and S. Newman, *J. Appl. Polym. Sci.*, **17,** 65 (1973).
12. M. Okubo, A. Yamada, and T. Matsumoto, *J. Polym. Sci., Polym. Chem. Ed.*, **16,** 3219 (1980).
13. M. Okubo, S. Yamaguchi, and T. Matsumoto, *J. Appl. Polym. Sci.*, **31,** 1075 (1986).
14. G. W. Poehlein, *Encyclopedia of Polymer Science and Engineering,* Wiley, New York, 1986, Vol. 6, p. 1.
15. A. Klien, *Kirk-Othmer Encyclopedia of Chemical Technology,* Wiley, New York, 1979, Vol. 14, p. 82.
16. J. W. Vanderhoff, *J. Polym. Sci., Polym. Symp.*, **72,** 161 (1985).
17. M. S. El-Aasser and J. W. Vanderhoff, *Emulsion Polymerization of Vinyl Acetate,* Applied Science London, 1981, p. 215.
18. E. B. Bradford and J. W. Vanderhoff, *J. Polym. Sci. C,* **3,** 41 (1963).
19. M. S. El-Aasser, T. Makgawinata, and J. W. Vanderhoff, *J. Polym. Sci., Polym. Chem. Ed.*, **21,** 2363 (1983).
20. S. C. Misra, C. Pichot, M. S. El-Aasser, and J. W. Vanderhoff, *J. Polym. Sci., Polym. Chem. Ed.*, **21,** 2383 (1983).
21. M. S. Silverstein and M. Narkis, *Polym. Eng. Sci.*, **29,** 824 (1989).
22. M. S. Silverstein, Y. Talmon, and M. Narkis, *Polymer,* **30,** 416 (1989).
23. M. S. Silverstein and M. Narkis, in *Advances in Interpenetrating Polymer Networks,* D. Klempner and K. C. Frisch, Eds., Technomic, Lancaster, PA, 1989.
24. M. S. Silverstein and M. Narkis, *Polym.-Plast. Technol. Eng.*, **26,** 271 (1987).
25. M. S. Silverstein and M. Narkis, *J. Appl. Polym. Sci.*, **33,** 2529 (1987).
26. F. A. Bovey, I. M. Kolthoff, A. I. Medalia, and E. J. Meehan, *Emulsion Polymerization,* Interscience, New York, 1955.
27. J. L. Gardon, *Rubber Chem. Technol.*, **43,** 74 (1970).
28. M. Narkis, Y. Talmon, and M. S. Silverstein, *Polymer,* **26,** 1359 (1985).
29. Y. Talmon, M. Narkis, and M. S. Silverstein, *J. Electron Microsc. Technique,* **2,** 589 (1985).
30. R. A. Steinbrecht and K. Zierold, *Cryotechniques in Biological Electron Microscopy,* Springer-Verlag, Berlin, 1987, p. 64.
31. Y. Talmon, M. Adrian, and J. Dubochet, *J. Microsc.*, **141,** 375 (1986).
32. M. Okubo, Y. Katsuta, and T. Matsumoto, *J. Polym. Sci., Polym. Lett. Ed.*, **20,** 45 (1982).
33. L. J. Hughes and G. L. Brown, *J. Appl. Polym. Sci.*, **7,** 59 (1963).
34. T. I. Min, A. Klein, M. S. El-Aasser, and J. W. Vanderhoff, *J. Polym. Sci., Polym. Chem. Ed.*, **21,** 2845 (1983).
35. S. L. Rosen, *J. Appl. Polym. Sci.*, **17,** 1805 (1973).
36. M. S. Silverstein and M. Narkis, *Polym. Eng. Sci.*, **25,** 257 (1985).
37. Y. Aoki, *J. Non-Newt. Fluid Mech.*, **2,** 91 (1986).
38. R. C. Penwell and R. S. Porter, *J. Appl. Polym. Sci.*, **13,** 2427 (1969).
39. R. C. Penwell and R. S. Porter, *J. Polym. Sci. A-2,* **9,** 463 (1971).

Received May 23, 1988
Accepted June 20, 1988